IBRO Neuroscience Reports 16 (2024) 560–566

Contents lists available at ScienceDirect

IBRO Neuroscience Reports

journal homepage: www.sciencedirect.com/journal/IBRO-Neuroscience-Reports

Research Paper

Developing preclinical dog models for reconstructive severed spinal cord continuity via spinal cord fusion technique

Tingting Shen [a,b,c,d,1], Weihua Zhang [b,c,d,1], Rongyu Lan [b,c,d], Zhihui Wang [a,b,c,d], Jie Qin [b,c,d], Jiayang Chen [a,b,c,d], Jiaxing Wang [b,c,d,e], Zhuotan Wu [a,b,c,d], Yangyang Shen [a,b,c,d], Qikai Lin [a,b,c,d], Yudong Xu [a,b,c,d], Yuan Chen [a,b,c,d], Yi Wei [a,b,c,d], Yiwen Liu [d,f], Yuance Ning [d,g], Haixuan Deng [h], Zhenbin Cao [h], Xiaoping Ren [a,b,c,d,e,*]

[a] Guangxi University of Chinese Medicine, Nanning, Guangxi 530001, China
[b] Department of Orthopedics, Ruikang Hospital Affiliated to Guangxi University of Chinese Medicine, Nanning, Guangxi 530011, China
[c] Institute of Orthopedics, Ruikang Hospital Affiliated to Guangxi University of Chinese Medicine, Nanning, Guangxi 530011, China
[d] Global Initiative to Cure Paralysis (GICUP Alliance), Columbus, OH 43221, United States
[e] Department of Medicine School, Guangxi University, Nanning, Guangxi 530004, China
[f] Department of Anatomy and Cell Biology, McGill University, Montreal, Quebec H3A 0G4, Canada
[g] Department of Pharmacology and Toxicology, University of Toronto, Toronto, Ontario M5S 1A8, Canada
[h] Department of Imaging, Ruikang Hospital Affiliated to Guangxi University of Chinese Medicine, Nanning, Guangxi 530011, China

ARTICLE INFO

Keywords:
Spinal cord injury
Spinal cord fusion
Polyethylene glycol
Spinal cord transplantation
Surgical procedure

ABSTRACT

Background: Spinal cord injury (SCI) is a severe impairment of the central nervous system, leading to motor, sensory, and autonomic dysfunction. The present study investigates the efficacy of the polyethylene glycol (PEG)-mediated spinal cord fusion (SCF) techniques, demonstrating efficacious in various animal models with complete spinal cord transection at the T10 level. This research focuses on a comparative analysis of three SCF treatment models in beagles: spinal cord transection (SCT), vascular pedicle hemisected spinal cord transplantation (vSCT), and vascularized allograft spinal cord transplantation (vASCT) surgical model.

Methods: Seven female beagles were included in the SCT surgical model, while four female dogs were enrolled in the vSCT surgical model. Additionally, twelve female dogs underwent vASCT in a paired donor-recipient setup. Three surgical model were evaluated and compared through electrophysiology, imaging and behavioral recovery.

Results: The results showed a progressive recovery in the SCT, vSCT and vASCT surgical models, with no statistically significant differences observed in cBBB scores at both 2-month and 6-month post-operation (both $P>0.05$). Neuroimaging analysis across the SCT, vSCT and vASCT surgical models revealed spinal cord graft survival and fiber regrowth across transection sites at 6 months postoperatively. Also, positive MEP waveforms were recorded in all three surgical models at 6-month post-surgery.

Conclusion: The study underscores the clinical relevance of PEG-mediated SCF techniques in promoting nerve fusion, repair, and motor functional recovery in SCI. SCT, vSCT, and vASCT, tailored to specific clinical characteristics, demonstrated similar effective therapeutic outcomes.

1. Introduction

Spinal cord injury (SCI) constitutes a severe impairment of the central nervous system, leading to motor, sensory, and autonomic dysfunction below the injury site (Hamid et al., 2018; Ahuja et al., 2017). The consequential disruption of nerve circuits results in unfavorable local inhibitory microenvironments characterized by limited nerve regeneration, cavomyelia, glial scar formation, inflammatory responses, and the release of axon growth inhibiting substances (Ahuja et al., 2017; Zhang et al., 2021). SCI has always been a research hotspot

* Correspondence to: Department of Orthopedics, Ruikang Hospital Affiliated to Guangxi University of Chinese Medicine, Huadong Road 10, Xingning District, Nanning, Guangxi 530011, China.
E-mail address: chinarenxg@126.com (X. Ren).
[1] First co-author.

https://doi.org/10.1016/j.ibneur.2024.04.006
Received 11 February 2024; Received in revised form 25 April 2024; Accepted 26 April 2024
Available online 29 April 2024

in the field of neural regeneration and repair. Existing approaches to SCI repair predominantly involve stem cell therapy (Zipser et al., 2022; Zipser et al. nd), tissue engineering scaffolds (Koffler et al., nd; Liu et al., nd), bioactive substances (Álvarez et al), and so on. Although there have been certain advancements in the treatment of SCI, it remains a highly complex medical issue. Our research team, in collaboration with international partners, introduced a polyethylene glycol (PEG)-mediated spinal cord fusion (SCF) technique in 2013 (Canavero and Ren, 2016; Ren et al., 2019a; Canavero et al., 2016). This technique utilizes a precise cutting tool to minimize spinal cord damage, creating two closely aligned sections for immediate local fusion with PEG. Applied in various animal models, including mice (Ye et al., 2016), rats (Ren et al., 2017), beagles (Liu et al., 2018; Ren et al., 2019b), and monkeys (Ren and Canavero, 2020), SCF has demonstrated varying degrees of restored hind limb function following acute SCI at the T10 level, characterized by a severity grade A of the American Spinal Injury Association (ASIA) classification (Kirshblum et al., 2019). Independent verification by Kim et al. confirmed SCF's effectiveness in complete cervical spinal cord transection models in mice (Kim et al., 2016a), rats (Kim et al., 2016b), and dogs (Kim et al., 2016c).

Our current research focuses on three distinct SCF treatment models in beagles: the spinal cord transection (SCT) surgical model (Liu et al., 2018; Ren et al., 2019b), the vascular pedicle hemisected spinal cord transplantation (vSCT) surgical model (Ren et al., 2021), and the vascularized allograft spinal cord transplantation (vASCT) surgical model. Each model demonstrated the ability to restore limb motor function post-surgery. However, a critical question emerges: do variations in therapeutic efficacy exist among these procedures? To address this, our study aims to compare the outcomes associated with these surgical interventions. By undertaking seeks to systematically compare and quantify the differential effects of the three SCF models, our objective is to contribute to the refinement of SCF protocols in clinical trials, ultimately fostering advancements in SCI patient treatment outcomes.

2. Materials and methods

2.1. Animal

In this study, a total of twenty-three female beagles, weighing about 8 kg. Animals were randomized into experimental groups using a computer-generated random number sequence generated by an independent researcher. Seven female beagles were included in the SCT surgical model, while four female dogs were enrolled in the vSCT surgical model. Twelve beagles were randomly paired, resulting in 6 pairs (one donor paired with one recipient). These 6 pairs dogs underwent vASCT surgical model. All procedures conducted in this study received approval from both the Institutional Animal Care and Use Committee of Harbin Medical University (HMUIRB-2008–06) and Animal Care and Use Committee of Guangxi University of Chinese Medicine (DW20230525–089). These procedures were carried out in strict accordance with Directive 2010/63/EU of the European Parliament. Moreover, the reporting of animal data adhered to The ARRIVE 2.0 guidelines (Kilkenny et al., 2010). The beagles utilized in this study were sourced from Qingdao Agricultural University and Guangzhou General Institute of Medical Research Co. LTD and were provided with comfortable living conditions, including a 12-hour light and dark cycle. Additionally, they had access to food and water ad libitum.

2.2. SCF procedure

2.2.1. SCT surgical model

In the experimental SCT surgical model, seven female beagles were included and subjected to PEG treatment. Prior to anesthesia induction, atropine (0.025 mg/kg) was administered intramuscularly as an anticholinergic agent. General anesthesia was induced with intramuscular ketamine (5 mg/kg) and intravenous propofol (4 mg/kg), followed by intubation and mechanical ventilation. Anesthesia was maintained with continuous intravenous propofol infusion (10 mg/kg/h) and remifentanil infusion (0.2 μg/kg/min) for analgesia. Intramuscular vecuronium (0.1 mg/kg) was given for muscle relaxation. The surgical procedure began with a precise incision in the skin and muscles covering the thoracic spinal column, followed by a T10 laminectomy using conventional neurosurgical instruments. Utilizing a surgical microscope, precision was maintained as the dura mater was meticulously opened, and the spinal cord was gently elevated using a Kirchner wire hook. Subsequently, the spinal cord was accurately transected with an ultrasharp microsurgical blade. Following transection, the animals were designated to undergo end-to-end fusion at the transection site through the application of topical PEG-600 (100%, Sigma-Aldrich/Merck) (2 ml), administered via a syringe. The procedure concluded with the implementation of standard layer-by-layer closure techniques as previously described (Liu et al., 2018; Ren et al., 2019b). Postoperatively, dogs were given cefoperazone sodium and sulbactam sodium IV solution (25 mg/kg; Harbin General Pharmaceutical Factory's Sales Company, Harbin, Heilongjiang, PRC) for three consecutive days. Additionally, dogs were administered meloxicam (Qilu Animal Health Products Co., Ltd, Jinan, Shandong, PRC) at 0.2 mg/kg intramuscularly once a day postoperatively until the dogs exhibited signs of pain relief. Their urine was manually expressed twice daily until normal voiding returned. They were fed dog food with access to water, receiving intravenous hydration if needed in the first two weeks post-surgery. Hip massage and lower limb exercises were conducted four times daily for rehabilitation.

2.2.2. vSCT surgical model

Four female dogs were enrolled in the vSCT surgical model. Before inducing anesthesia, atropine was administered intramuscularly at a dose of 0.025 mg/kg as an anticholinergic agent. General anesthesia was initiated with intramuscular ketamine at 5 mg/kg and intravenous propofol at 4 mg/kg, followed by intubation and mechanical ventilation. Anesthesia was maintained using continuous intravenous infusions of propofol at 10 mg/kg/h and remifentanil at 0.2 μg/kg/min for pain relief. Intramuscular vecuronium was administered at a dose of 0.1 mg/kg for muscle relaxation. A laminectomy was meticulously performed at the T10-T11 spinal level, exposing the spinal cord. A precise 1 cm segment of the spinal cord at T10 was then removed, creating a gap through sharp transection using an ultrasharp microsurgical blade. Subsequently, one portion of the spinal cord, including half of its tissue and one side of the posterior spinal artery, was meticulously excised either from the lower or upper spinal cord region. This segment was then transplanted to bridge the gap between the lower and upper spinal cord stumps, ensuring the arterial supply remained intact. The remaining side of the posterior spinal artery served as the vascular connection to sustain blood flow to the transplanted spinal cord tissue. At the autotransplantation site, dogs were treated with PEG 600 (2 ml) for 5 minutes. Subsequent to the treatment, standard closure procedures were meticulously implemented layer by layer as previously studied (Ren et al., 2021). Following the above procedures, all dogs received intravenous cefoperazone sodium and sulbactam sodium IV solution (25 mg/kg; Harbin General Pharmaceutical Factory's Sales Company, Harbin, Heilongjiang, PRC) for three consecutive days. Moreover, dogs were given meloxicam (0.2 mg/kg; Qilu Animal Health Products Co., Ltd, Jinan, Shandong, PRC) intramuscularly once a day after surgery until they showed signs of pain relief. Urine was manually expelled from the bladder twice daily until the dogs regained their normal voiding reflex. They had access to water and received intravenous electrolyte solutions if unable to consume food or water during the initial postoperative week. Four times daily, each SCI dog underwent lower limb rehabilitation with range-of-motion exercises and hip massages. Additionally, the dogs were supported by a custom wheelchair-like device to aid mobility and prevent pressure sores and skin irritations until voluntary motor function improved.

2.2.3. vASCT surgical model

In this study, 12 female dogs underwent vASCT in a paired donor-recipient setup. The dogs were first administered dexmedetomidine (Nanjing Zhengda Tianqing Pharmaceutical Co. LTD, Nanjing, China) at a dose of 5 μg/kg intramuscularly for sedation, assisted by mechanical ventilation. Subsequently, propofol was administered at a dose of 3–5 mg/kg for anesthesia induction, maintained with 1.5% isoflurane (Rayward Life Technology Co., LTD, Shenzhen, China). Fentanyl citrate (Yichang Renfu Pharmaceutical Co. LTD, Yichang, China) was administered at a rate of 10 μg/kg/h for analgesia. The donor phase involved precise incisions at the T9-T11 levels to isolate the spinal cord tissue along with the radicular artery (RA) - dorsal intercostal artery (DIA) and accompanying vein at the T10 level serving as its vascular pedicle. Microscopic guidance and specialized microinstruments ensured the careful extraction and preservation of the spinal cord tissue, which was then enveloped in ice-cold saline-soaked gauze. Subsequently, the donor dog underwent euthanasia via intravenous injection of a euthanasia solution containing propofol (10 mg/kg) and potassium chloride injection (0.2 g/kg), in accordance with established ethical and scientific protocols. Simultaneously, in the recipient phase, a separate group of surgeons operated on recipient beagles, creating longitudinal incisions at the T9-T11 levels. Vascular reconstruction is a priority, and the vascular pedicle (including the RA-DIA and accompanying vein) of the donor spinal cord graft was meticulously anastomosed end-to-end with the muscle perforator and vein of the recipient DIA. The mean cold ischemia time of donor spinal cord was about 2 hours. After the donor spinal cord re-established blood circulation, a precise 1.5 cm spinal cord defect was created at the T10 level from the recipient dog. A tunnel was crafted between paraspinal muscles to facilitate transplantation, and the donor spinal cord graft was meticulously bridged at both distal and proximal stumps of the recipient spinal cord with the local application of 2 ml PEG. The procedure included suturing the dura mater to prevent cerebrospinal fluid leakage and a layer-by-layer closure of the incision. Subsequent to the surgical intervention, the recipient beagles underwent a treatment regimen designed to prevent immune rejection, which included the oral administration of tacrolimus (Hangzhou Sino-American East China Pharmaceutical Co., LTD, Hangzhou, China) at a dosage of 0.2 mg/kg/day (Udina et al., nd) for six months. In addition, intramuscular injections of methylprednisolone sodium succinate (Liaoning HAISCO Pharmaceutical Co. LTD, Xingcheng, China) were administered at a dosage of 1.0 mg/kg/day for 7 days following the surgical procedures. Also, the study involved administering 25 mg/kg/day of ceftriaxone sodium (Shanghai Roche Pharmaceutical Co., LTD, Shanghai, China) and 100 IU/kg/day of heparin (Maanshan Fengyuan Pharmaceutical Co., LTD, Maanshan, China) to all participating beagles for 7 days post-surgery. Furthermore, dogs received intramuscular administration of meloxicam (0.2 mg/kg; Qilu Animal Health Products Co., Ltd, Jinan, Shandong, PRC) once daily following surgery until they displayed indications of pain alleviation. Besides, the dogs received assistance with defecation and urination through abdominal massage three times daily until their voiding reflex returned. Daily passive movement of hind limb joints and buttocks massage were conducted to prevent stiffness and pressure sores. Beagles were also provided with custom-made support akin to a wheelchair to aid mobility until significant voluntary motor function recovery occurred, crucial for preventing pressure sores and skin irritations.

2.3. Locomotor function assessment

Two proficient examiners conducted systematic and comprehensive assessments on all the beagles to monitor the recovery of hind limb function over 5-minute intervals at specific time points: 3, 10, 17, 24, 31, 38, 45, 52, 59, and 180 days postoperatively. The evaluations were executed using the canine Basso-Beattie-Bresnahan rating scale (cBBB) (Song et al., 2016), where a cBBB score of 0 signifies paraplegia, and a score of 19 denotes normal function. This rating scale serves as a precise metric for objectively assessing the movement, coordination, and overall stability of the hind limbs in the beagles. This methodology ensures a rigorous and standardized approach to objectively measure and document the progress of hind limb recovery in the experimental subjects.

2.4. Neuroimaging examination

All animals underwent magnetic resonance imaging (MRI) and diffusion tensor imaging (DTI) procedures using a 1.5 Tesla MRI system (Achieva Magnetic Resonance System, Philips, Amsterdam, The Netherlands). For MRI, sagittal T2-weighted fast spin-echo sequences were employed with parameters set at TR = 1700 ms, TE = 100 ms, slice thickness = 3 mm, slice gap = 0.1, and NSA = 4. Additionally, axial single-shot echo-planar DTI sequences were utilized with parameters set at TR = 6100 ms, TE = 93 ms, voxel size = 2 mm × 2 mm, slice thickness = 2 mm, slice gap = 0, NSA = 2, and 15 diffusion directions. Both MRI and DTI were performed at 6 months postoperatively, for all animals.

2.5. Electrophysiological detection

Six months post-surgery, a postoperative electrophysiological assessment, specifically involving Motor Evoked Potentials (MEPs), was conducted. MEPs were elicited through the application of brief transcranial electrical pulses, featuring a pulse width of 75 μs and a high voltage of 150 V in an anodal electrical stimulus train. The stimulating electrodes were precisely positioned over the motor cortex regions at C3 and C4, adhering to the international 10–20 EEG system. Concurrently, the recording electrodes were strategically placed at the tibialis anterior in the lower extremities.

2.6. Statistical analysis

The statistical analysis was conducted using SPSS 26.0 (IBM Inc., SPSS Statistics, Armonk, NY, USA) and GraphPad Prism 7 (GraphPad Software, La Jolla, CA, USA) for both statistical analysis and graphical representation purposes. Prior to analysis, normality of data distributions was assessed using Kolmogorov-Smirnov tests. Motor assessments (cBBB scores) underwent analysis through one-way analysis of variance (ANOVA) and Kruskal-Wallis H-test. Meanwhile, the latency and amplitude of electrophysiology assessments were analyzed by one-way ANOVA. For one-way ANOVA analyses, a Tukey post-hoc test was employed to identify paired differences among groups. In cases where the Kruskal-Wallis H test was used, the Bonferroni correction method for pairwise comparison was applied to indicators with significant differences. Statistical significance was determined at a bilateral p-value threshold of less than 0.05.

3. Results

3.1. Functional recovery

Before spinal cord transection, all animals exhibited normal cBBB scores (score: 19), and complete paraplegia (score: 0) postoperatively. In the SCT surgical model, seven dogs demonstrated initial signs of recovery within three days, characterized by twitching in both hind limbs in response to light pinching of the abdominal wall. The vSCT surgical model showed one dog with the first signs of motor recovery (autonomous hindlimb movement) at 17 days post-operation, while the vASCT surgical model had two beagles displaying voluntary hind limb movement (scoring one) at 12 days post-surgery. Unfortunately, one beagle within the SCT group unexpectedly succumbed to complications arising from anesthesia. In contrast, within the vASCT group, three beagles exhibited mild gastrointestinal reactions, manifesting symptoms such as anorexia, diarrhea, weight loss, and other related gastrointestinal issues. Conversely, no associated complications were observed in the vSCT group during both the postoperative period and subsequent follow-up.

Throughout each model, recovery was consistently progressive without plateaus, showing gradual improvement over time (Table 1, Fig. 1). Significant differences in cBBB scores were observed among the SCT, vSCT, and vASCT surgical models at post-operation intervals of 3, 10, 17, and 24 days ($p<0.05$, as depicted in Table 1 and Fig. 1). Conversely, no substantial variations in cBBB scores were discerned among the SCT, vSCT, and vASCT surgical models at 31, 38, 45, 52, 59, and 180 days post-operation ($p>0.05$, as illustrated in Table 1 and Fig. 1). These findings underscore the temporal dynamics of functional recovery following distinct surgical interventions, highlighting critical time points for therapeutic assessment.

3.2. Neuroimaging assessment

MRI and DTI examinations were employed for a comprehensive assessment of spinal cord neural continuity following surgery. At the 6-month post-operation mark, T2-weighted MRI scans indicated increased re-establishment of anatomic tissue continuity across the graft site in SCT-treated, vSCT-treated and vASCT-treated dogs. Also, DTI showed continued fiber regrowth across the transection plane in the three surgical models (Fig. 2). Visual inspection through tractography revealed a correlation between the extent of cord reconnection and behavioral recovery, with near-normal dogs displaying almost normal cords in these groups.

3.3. Electrophysiology assessment

In this research, MEP were evaluated in dogs undergoing SCT, vSCT, and vASCT as illustrated in Fig. 3. Before the surgical procedures, normal MEP waveforms were recorded in the tibialis anterior of the lower extremities. Following the transection, the normal MEP waveform disappeared in all three surgical models. Six months post-surgery, positive MEP waveforms were recorded in all three groups of postoperative beagles. Notably, compared to the SCT group, the vSCT and vASCT groups exhibited prolonged MEP latency and lower amplitude. Furthermore, beagle dogs in the vASCT group displayed higher amplitude compared to those in the vSCT group.

The latency and amplitude in the electrophysiology assessment was shown in Table 2. Before surgery, there were no significant differences in latency and amplitude among the SCT group, vSCT group, and vASCT group ($P>0.05$). However, at 6 months postoperatively, significant differences were observed in latency and amplitude among the three groups ($P<0.05$). Additionally, the latency and amplitude of the SCT group showed significant differences compared to the vSCT group and vASCT group ($P<0.05$). However, there were no significant differences in latency and amplitude between the vSCT group and vASCT group ($P>0.05$).

4. Discussion

In this study, the results collectively suggest that all three surgical approaches—SCT, vSCT, and vASCT—demonstrate the potential to partially restore motor function in beagles afflicted with complete SCI. This assertion is substantiated by the re-establishment of anatomical continuity and the restoration of electrical signal transmission within the damaged spinal cord. The study implies that the choice of surgical approach should be based on considerations such as surgical feasibility, patient-specific factors, and potential ancillary benefits, as all three approaches demonstrated similar benefits in achieving the desired therapeutic outcomes.

The findings of this study provide valuable insights into the motor functional recovery, neuroimaging and electrophysiology assessments, following three distinct SCF surgical models—SCT, vSCT, and vASCT—in a canine model. SCT, vSCT, and vASCT all belong to PEG-mediated SCF, while the key to a successful SCF depends on the application of precision surgical techniques and fusion agents. Firstly,

Table 1
The cBBB scores in the SCT, vSCT, and vASCT surgical models at different time points.

Days	SCT surgical model							Median	vSCT surgical model				Median	vASCT surgical model						Median	F/H	*P1*	*P2*	*P3*	*P4*
	S1	S2	S3	S4	S5	S6	S7		S1	S2	S3	S4		S1	S2	S3	S4	S5	S6						
-1	19	19	19	19	19	19	19	19	19	19	19	19	19	19	19	19	19	19	19	19	NA	NA	NA	NA	NA
0	0	0	0	0	0	0	0	0	0	0	0	0	0	0	0	0	0	0	0	0	NA	NA	NA	NA	NA
3	1	1	2	2	2	2	1	2	0	0	0	0	0	0	0	0	0	0	0	0	41.52	0.001	0.007	0.002	1
10	4	2	5	4	4	2	2	4	0	0	0	0	0	0	0	0	0	0	0	0	33.004	0.001	0.007	0.002	1
17	5	2	9	5	6	6	3	5	0	0	1	0	0.5	1	3	3	3	0	0	2	11.756	0.001	0.001	0.008	0.443
24	9	7	9	5	6	6	3	6	1	0	4	4	2.5	3	3	7	3	1	0	3	6.179	0.012	0.024	0.029	0.914
31	9	7	9	5	6	6	3	6	7	4	6	6	5	4	3	7	6	1	0	3.5	3.521	0.088	0.88	0.081	0.295
38	10	7	10	6	5	6	3	6	9	8	7	9	8.5	7	3	8	5	3	1	4	3.231	0.07	0.565	0.243	0.066
45	10	7	10	7	6	6	3	7	10	8	9	10	9.5	7	3	8	7	6	6	6.5	3.067	0.079	0.194	0.729	0.069
52	12	8	12	7	6	7	3	7	12	8	10	11	10.5	10	3	8	8	6	6	7	1.986	0.174	0.355	0.775	0.155
59	15	8	18	9	7	7	5	8	12	9	10	12	11	11	7	8	8	6	10	8	0.665	0.53	0.908	0.704	0.527
180	18	10	18	12	NA	10	7	11	12	11	10	12	11.5	14	14	10	10	10	10	10	0.333	0.879	NA	NA	NA

P1: Comparison among three groups; P2: Comparison between the vSCT group and the SCT group; P3: Comparison between the vASCT group and the SCT group; P4: Comparison between the vASCT group and the vSCT group.

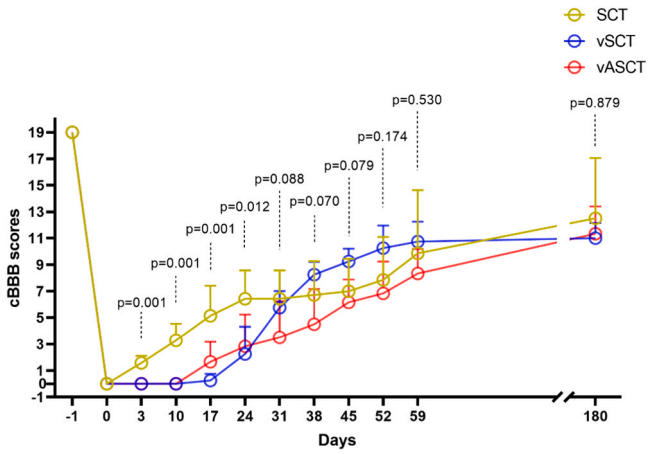

Fig. 1. cBBB scores. The cBBB scores in the SCT, vSCT, and vASCT surgical models at different time points. The recovery of motor function in the three groups showed an upward trend over time. Significant differences in cBBB scores were observed among the SCT, vSCT, and vASCT surgical models at 3, 10, 17 and 24-day post-operation ($p<0.05$), while no significant differences in cBBB scores were revealed among the SCT, vSCT, and vASCT surgical models at 31, 38, 45, 52, 59 and 180-day post-operation ($p>0.05$).

achieving successful SCF hinges on the executing precision of an extremely sharp cross-cut on the spinal cord, crucial for minimizing damage to local gray and white matter. The applied force, kept below 10 newtons, stands in stark contrast to the approximately 26,000 newtons encountered in clinical SCIs, a 2,600-fold difference (Sledge et al., 2013). In SCF, the ultramicroscopic blade's specific shape, crafted from carbon nanotubes, enables nanoscale-level crosscutting, reducing axial mutations (Chang et al., 2010; Reibold et al., 2006; Reyssat et al., 2012). This method ensures a thin-cell layer transection, minimizing damage and facilitating immediate re-sprouting of inherent nerve fibers in the gray matter neurofiber network (Canavero and Ren, 2016). Thus, the key to SCF success lies in creating a fresh, sharp transected spinal cord incision, followed by a meticulous alignment of the proximal and distal ends with no gap, promoting optimal healing conditions. Secondly, PEG, known for its stability, non-toxicity, and biocompatibility, proves effective in fusing cell membranes, inducing membrane resealing, diminishing oxidative stress and providing essential energy support, which plays a neuroprotective and reparative function in SCI (Ren et al., 2019a; Kong et al., 2017; Lu et al., 2018; Shi, 2013). Noteworthy is the critical application time of PEG, as the spinal cord neurons remains stable for only about 10–20 minutes before rupture, and these severed neurons spans only 0.3 mm, surviving stably for 3–7 days, with approximately 30% of proximal axons regenerating within 6–24 h (Canavero and Ren, 2016; Canavero et al., 2016, 2017). Consequently, the application of PEG to the broken spinal cord junction within a few minutes (less than 10 minutes) is imperative. Besides, although PEG can

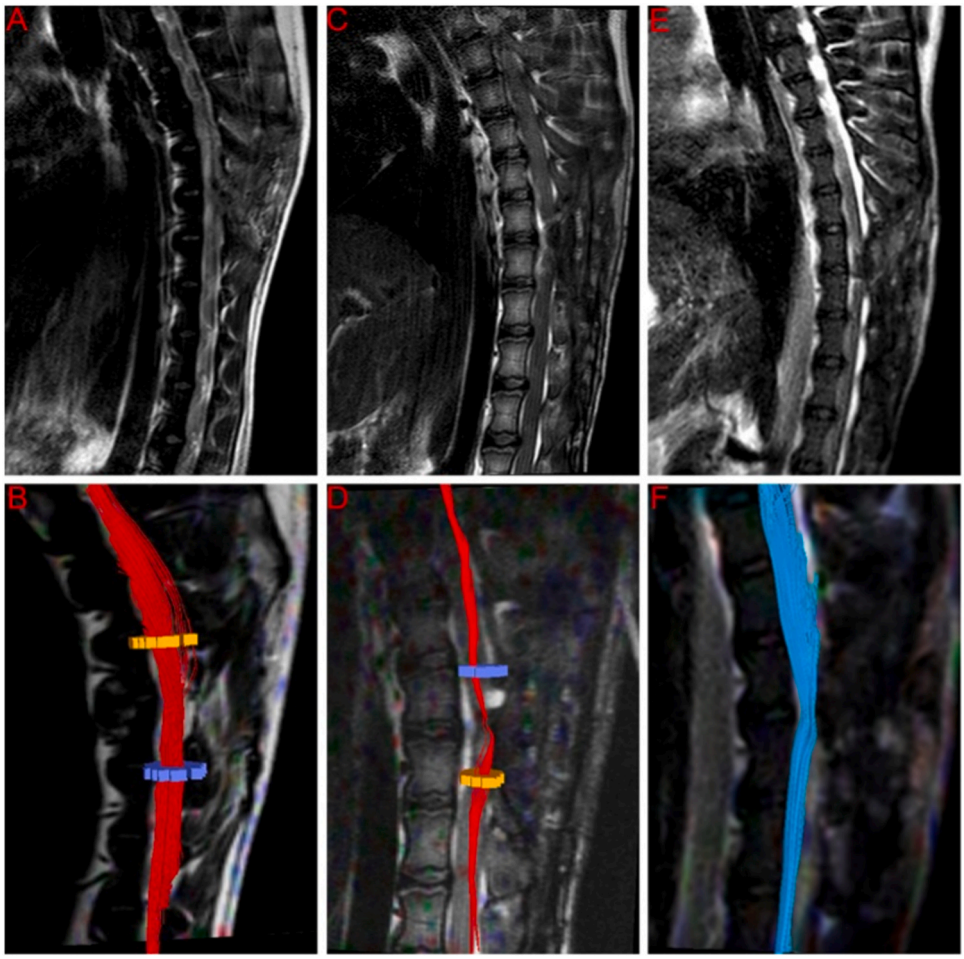

Fig. 2. T2W and DTI at 6-month post-operation. T2-weighted MRI scans indicated increased re-establishment of anatomic tissue continuity across the graft site in SCT-treated (A), vSCT-treated (C) and vASCT-treated (E) dogs. DTI showed continued fiber regrowth across the transection plane in the SCT (B), vSCT (D) and vASCT (F) surgical models.

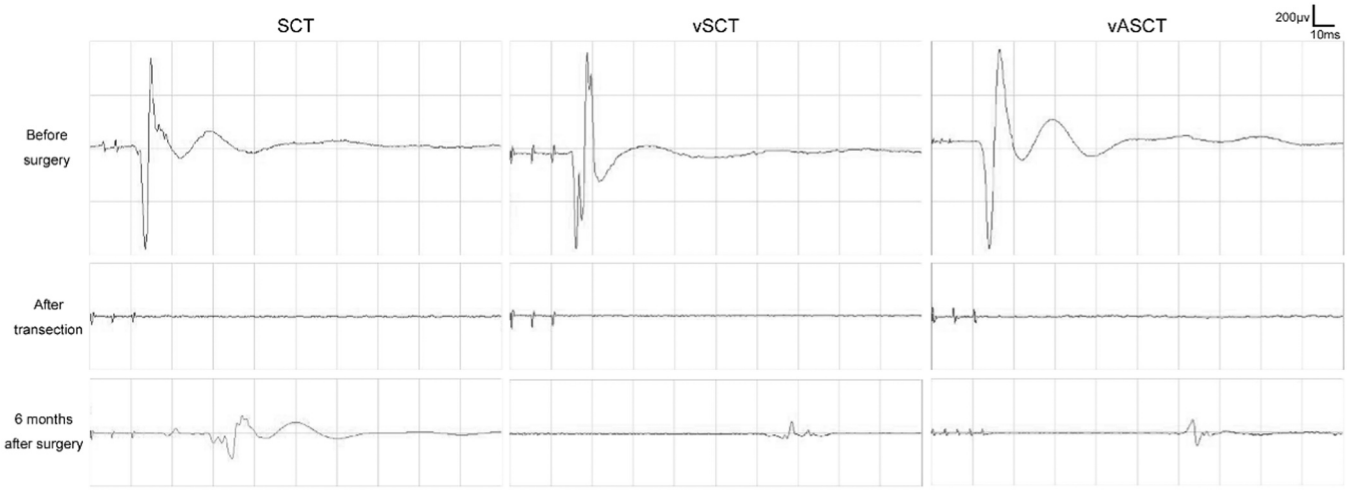

Fig. 3. MEP examination in the SCT, vSCT, and vASCT surgical models. Positive MEP waveforms were recorded in all three groups after operation, but the latency and amplitude were prolonged and lower to varying degrees compared with those before operation.

Table 2
The latency and amplitude in the electrophysiology assessment.

Groups	SCT	vSCT	vASCT	*P1*	*P2*	*P3*	*P4*
Before surgery							
Latency(ms)	12.79±1.48	12.60±1.64	12.63±0.85	0.968	0.973	0.977	0.999
Amplitude(μv)	683.86±167.18	608.90±175.53	553.57±243.84	0.514	0.823	0.487	0.904
6 months after surgery							
Latency(ms)	32.13±4.58	62.85±3.38	58.53±2.79	<0.001	<0.001	<0.001	0.206
Amplitude(μv)	121.07±25.88	76.03±15.89	88.90±10.95	0.006	0.007	0.030	0.561

P1: Comparison among three groups;
P2: Comparison between the vSCT group and the SCT group;
P3: Comparison between the vASCT group and the SCT group;
P4: Comparison between the vASCT group and the vSCT group.

effectively fuse nerve axon membranes, mismatches occur when two spinal cord ends are fused. How many nerve fibers are actually fused to ensure limb movement? Previous studies in humans and animals indicate that maintaining 5–20% of these fibers is sufficient to achieve a satisfactory level of motor function, thus, PEG, with the capacity to fuse 10–15% of nerve fiber bundles, holds significant clinical relevance (Canavero et al., 2016; Basso, 2000; Canavero, 2015). Animal studies (mice (Ye et al., 2016; Kim et al., 2016a), rats (Ren et al., 2017; Kim et al., 2016b), dogs (Liu et al., 2018; Ren et al., 2019b; Kim et al., 2016c) and monkeys (Ren and Canavero, 2020)) also has substantiated the positive impact of PEG on motor function improvement in complete SCIs. Therefore, the integration of PEG-mediated SCF techniques, including SCT, vSCT, and vASCT, with the utilization of precision knives and the application of PEG as a membrane fusion agent, presents a comprehensive and promising strategy for accelerating nerve fusion, promoting repair, and enhancing functional recovery of locomotion in SCI.

SCT, vSCT, and vASCT represent distinct SCF surgical models developed for SCI, each tailored to specific clinical characteristics. SCT is primarily intended for patients with acute SCI resulting from sharp instrument injuries. Currently, the SCT surgical model has been verified in animal models of complete spinal cord transection in mice (Ye et al., 2016), rats (Ren et al., 2017) and beagles (Liu et al., 2018; Ren et al., 2019b). However, its applicability diminishes for those with common chronic SCI characterized by significant spinal cord defects. To address this limitation, the vSCT operation model was developed, specifically designed for patients with chronic SCI located in the thoracic segment without severe spinal atrophy. The vSCT model has been tested in beagles (Ren et al., 2021), demonstrating restored motor function and the re-establishment of anatomic continuity, along with interfacial axonal sprouting. Additionally, clinical population trials were conducted, and the results showed that in eight paraplegics treated with vSCT, objective improvements occurred in motor function for one individual, in autonomic nerve function in seven participants, and in symptoms of cord central pain for seven participants, in electrophysiologic motor-evoked potentials for one individual, in restoration of white matter continuity in three participants (Ren et al., 2022). Nevertheless, vSCT comes with limitations, as it doesn't apply to individuals with distal SCIs (such as those near the cauda equina nerve) or notable distal spinal cord atrophy. Introducing a more versatile approach, the vASCT model was formulated to accommodate both acute and chronic SCI patients with injuries spanning more than one spinal segment. Operationally, SCT involves the fusion of one spinal cord transeciton, whereas both vSCT and vASCT incorporate the fusion of two spinal cord transecitons, potentially influencing early postoperative functional recovery. Behavioral scores and cBBB scores for SCT indicate swifter recovery in the initial two months compared to the latter two methods, yet no substantial long-term motor function differences were observed at the six-month mark. Additionally, spinal cord transplantation is fundamental to both vSCT and vASCT. vSCT utilizes autogenous semi-spinal cord transplantation with a vascular pedicle, while vASCT entails allogeneic total spinal cord transplantation. Vascular reconstruction and the administration of long-term anti-immune rejection drugs are imperative for vASCT to reinstate blood circulation and prevent rejection of the allogeneic spinal cord graft.

While the study provides valuable insights, further research is warranted to explore the long-term effects and potential complications associated with each SCF surgical model. Additionally, investigating the underlying cellular and molecular mechanisms contributing to the observed functional and structural changes will enhance our

understanding of SCI repair strategies. In conclusion, this study contributes valuable information to the evolving field of SCI research, offering a basis for future investigations and clinical applications aimed at improving the prognosis and quality of life for individuals with SCI.

Ethical approval

All procedures conducted in this study received approval from both the Institutional Animal Care and Use Committee of Harbin Medical University (HMUIRB-2008–06) and Animal Care and Use Committee of Guangxi University of Chinese Medicine (DW20230525–089).

Funding

This work was supported by the National Natural Science Foundation of China (grant numbers 82060874) and the Science and Technology Department of Guangxi Zhuang Autonomous Region (grant numbers Guike AB21196062).

CRediT authorship contribution statement

Tingting Shen: Writing – review & editing, Writing – original draft, Methodology, Investigation, Formal analysis, Data curation. **Weihua Zhang**: Writing – review & editing, Visualization, Validation, Methodology, Investigation, Formal analysis, Data curation. **Rongyu Lan**: Writing – review & editing, Methodology, Investigation. **Zhihui Wang**: Writing – review & editing, Methodology, Investigation, Data curation. **Jie Qin**: Writing – review & editing, Methodology, Investigation. **Jiayang Chen**: Writing – review & editing, Investigation, Data curation. **Jiaxing Wang**: Writing – review & editing, Investigation, Data curation. **Zhuotan Wu**: Writing – review & editing, Investigation. **Yangyang Shen**: Writing – review & editing, Investigation, Data curation. **Qikai Lin**: Writing – review & editing, Investigation. **Yudong Xu**: Writing – review & editing, Investigation. **Yuan Chen**: Writing – review & editing, Investigation. **Yi Wei**: Writing – review & editing, Investigation. **Yiwen Liu**: Writing – review & editing, Data curation. **Yuance Ning**: Writing – review & editing, Data curation. **Haixuan Deng**: Writing – review & editing, Visualization, Data curation. **Zhenbin Cao**: Writing – review & editing, Visualization, Data curation. **Xiaoping Ren**: Writing – review & editing, Writing – original draft, Supervision, Project administration, Methodology, Funding acquisition, Conceptualization.

Declaration of Competing Interest

The authors of this manuscript have no conflicts of interest to disclose.

Data availability

The data that support the findings of this study are available from the corresponding author upon reasonable request.

References

Ahuja, C.S., Wilson, J.R., Nori, S., et al., 2017. Traumatic spinal cord injury, 2017/04/28 Nat. Rev. Dis. Prim. 3, 17018. https://doi.org/10.1038/nrdp.2017.18.

Álvarez Z., Kolberg-Edelbrock A.N., Sasselli I.R., et al. Bioactive scaffolds with enhanced supramolecular motion promote recove ry from spinal cord injury. Science; 374: 848-856. DOI: 10.1126/science.abh3602.

Basso, D., 2000. Neuroanatomical substrates of functional recovery after experimental spinal cord injury: implications of basic science research for human spinal cord injury. Phys. Ther. 80, 808–817.

Canavero, S., 2015. The "Gemini" spinal cord fusion protocol: reloaded, 2015/02/25 Surg. Neurol. Int 6, 18. https://doi.org/10.4103/2152-7806.150674.

Canavero, S., Ren, X., 2016. Houston, GEMINI has landed: spinal cord fusion achieved. Surg. Neurol. Int. 7, 626. https://doi.org/10.4103/2152-7806.190473.

Canavero, S., Ren, X., Kim, C.Y., et al., 2016. Neurologic foundations of spinal cord fusion (GEMINI). Surgery 160, 11–19. https://doi.org/10.1016/j.surg.2016.01.027.

Canavero, S., Ren, X., Kim, C.Y., 2017. Reconstructing the severed spinal cord. Surg. Neurol. Int. 8, 285. https://doi.org/10.4103/sni.sni_406_17.

Chang, W., Hawkes, E., Keller, C., et al., 2010. Axon repair: surgical application at a subcellular scale. Wiley Interdiscip. Rev. Nanomed. nanobiotechnology 2, 151–161. https://doi.org/10.1002/wnan.76.

Hamid, R., Averbeck, M.A., Chiang, H., et al., 2018. Epidemiology and pathophysiology of neurogenic bladder after spinal cord injury, 2018/05/13 World J. Urol. 36, 1517–1527. https://doi.org/10.1007/s00345-018-2301-z.

Kilkenny, C., Browne, W.J., Cuthill, I.C., et al., 2010. Improving Bioscience Research Reporting: the ARRIVE Guidelines for Reporting Animal Research. PLoS Biol. 8 https://doi.org/10.1371/journal.pbio.1000412.

Kim, C., Hwang, I., Kim, H., et al., 2016c. Accelerated recovery of sensorimotor function in a dog submitted to quasi-total transection of the cervical spinal cord and treated with PEG. Surg. Neurol. Int. 7, S637–S640. https://doi.org/10.4103/2152-7806.190476.

Kim, C., Oh, H., Hwang, I., et al., 2016a. GEMINI: Initial behavioral results after full severance of the cervical spinal cord in mice. Surg. Neurol. Int. 7, S629–S631. https://doi.org/10.4103/2152-7806.190474.

Kim, C.Y., Sikkema, W.K., Hwang, I.K., et al., 2016b. Spinal cord fusion with PEG-GNRs (TexasPEG): Neurophysiological recovery in 24 h in rats. Surg. Neurol. Int 7, S632–S636. https://doi.org/10.4103/2152-7806.190475.

Kirshblum S., Snider B., Rupp R., et al. Updates of the International Standards for Neurologic Classification o f Spinal Cord Injury: 2015 and 2019. Phys Med Rehabil Clin N Am; 31: 319-330. DOI: 10.1016/j.pmr.2020.03.005.

Koffler J., Zhu W., Qu X., et al. Biomimetic 3D-printed scaffolds for spinal cord injury repair. Nature medicine; 25: 263-269. DOI: 10.1038/s41591-018-0296-z.

Kong, X., Tang, Q., Chen, X., et al., 2017. Polyethylene glycol as a promising synthetic material for repair of spinal cord injury. Neural Regen. Res. 12, 1003–1008. https://doi.org/10.4103/1673-5374.208597.

Liu X., Hao M., Chen Z., et al. 3D bioprinted neural tissue constructs for spinal cord injury repair. Biomaterials; 272: 120771. DOI: 10.1016/j.biomaterials.2021.120771.

Liu, Z., Ren, S., Fu, K., et al., 2018. Restoration of motor function after operative reconstruction of the acutely transected spinal cord in the canine model, 2017/12/11 Surgery 163, 976–983. https://doi.org/10.1016/j.surg.2017.10.015.

Lu, X., Perera, T.H., Aria, A.B., et al., 2018. Polyethylene glycol in spinal cord injury repair: a critical review. J. Exp. Pharm. 10, 37–49. https://doi.org/10.2147/JEP.S148944.

Reibold, M., Paufler, P., Levin, A., et al., 2006. Materials: carbon nanotubes in an ancient Damascus sabre. Nature 444, 286. https://doi.org/10.1038/444286a.

Ren X. and Canavero S. The technology of head transplantation. New developments in medical research. New York: Nova Science Publishers, 2020, p. 1 online resource.

Ren, X., Kim, C.Y., Canavero, S., 2019a. Bridging the gap: spinal cord fusion as a treatment of chronic spinal cord injury. Surg. Neurol. Int. 10, 1–24. https://doi.org/10.25259/sni-19-2019.

Ren, S., Liu, Z., Kim, C.Y., et al., 2019b. Reconstruction of the spinal cord of spinal transected dogs with polyethylene glycol, 2019/09/19 Surg. Neurol. Int 10, 50. https://doi.org/10.25259/SNI-73-2019.

Ren, S., Liu, Z.H., Wu, Q., et al., 2017. Polyethylene glycol-induced motor recovery after total spinal transection in rats, 2017/06/15 CNS Neurosci. Ther. 23, 680–685. https://doi.org/10.1111/cns.12713.

Ren, S., Zhang, W., Liu, H., et al., 2021. Transplantation of a vascularized pedicle of hemisected spinal cord to establish spinal cord continuity after removal of a segment of the thoracic spinal cord: a proof-of-principle study in dogs. CNS Neurosci. Ther. https://doi.org/10.1111/cns.13696.

Ren, X., Zhang, W., Qin, J., et al., 2022. Partial restoration of spinal cord neural continuity via vascular pedicle hemisected spinal cord transplantation using spinal cord fusion technique, 2022/05/13 CNS Neurosci. Ther.. https://doi.org/10.1111/cns.13853.

Reyssat, E., Tallinen, T., Le Merrer, M., et al., 2012. Slicing softly with shear. Phys. Rev. Lett. 109, 244301 https://doi.org/10.1103/PhysRevLett.109.244301.

Shi, R., 2013. Polyethylene glycol repairs membrane damage and enhances functional recovery: a tissue engineering approach to spinal cord injury, 2013/07/31 Neurosci. Bull. 29, 460–466. https://doi.org/10.1007/s12264-013-1364-5.

Sledge, J., Graham, W.A., Westmoreland, S., et al., 2013. Spinal cord injury models in non human primates: are lesions created by sharp instruments relevant to human injuries?, 2013/08/21 Med. Hypotheses 81, 747–748. https://doi.org/10.1016/j.mehy.2013.07.040.

Song, R.B., Basso, D.M., da Costa, R.C., et al., 2016. Adaptation of the Basso-Beattie-Bresnahan locomotor rating scale for use in a clinical model of spinal cord injury in dogs. J. Neurosci. Methods 268, 117–124. https://doi.org/10.1016/j.jneumeth.2016.04.023.

Udina E., Ceballos D., Verdú E., et al. Bimodal dose-dependence of FK506 on the rate of axonal regeneration in mouse peripheral nerve. Muscle Nerve; 26: 348-355. DOI: 10.1002/mus.10195.

Ye, Y., Kim, C.Y., Miao, Q., et al., 2016. Fusogen-assisted rapid reconstitution of anatomophysiologic continuity of the transected spinal cord. Surgery 160, 20–25. https://doi.org/10.1016/j.surg.2016.03.023.

Zhang, Y., Al Mamun, A., Yuan, Y., et al., 2021. Acute spinal cord injury: pathophysiology and pharmacological intervention (Review). Mol. Med. Rep. 23 https://doi.org/10.3892/mmr.2021.12056.

Zipser C.M., Cragg J.J., Guest J.D., et al. Cell-based and stem-cell-based treatments for spinal cord injury: evid ence from clinical trials. The Lancet Neurology; 21: 659-670. DOI: 10.1016/S1474-4422(21)00464-6.

Zipser, C., Cragg, J., Guest, J., et al., 2022. Cell-based and stem-cell-based treatments for spinal cord injury: evidence from clinical trials. Lancet Neurol. 21, 659–670. https://doi.org/10.1016/s1474-4422(21)00464-6.